Selective Reduction of fMRI Responses to Transient Achromatic Stimuli in the Magnocellular Layers of the LGN and the Superficial Layer of the SC Of Early Glaucoma Patients

Peng Zhang,[1]* Wen Wen,[2] Xinghuai Sun,[2]* and Sheng He[1,3]

[1]*State Key Laboratory of Brain and Cognitive Science, Institute of Biophysics, Chinese Academy of Sciences, Beijing, China*
[2]*Department of Ophthalmology, Eye and ENT Hospital, Fudan University, Shanghai, China*
[3]*Department of Psychology, University of Minnesota, Minneapolis, Minnesota*

◆━━━━━━━━━━━━━━━━━━━━━━━━━━━━━━◆

Abstract: Glaucoma is now viewed not just a disease of the eye but also a disease of the brain. The prognosis of glaucoma critically depends on how early the disease can be detected. However, early glaucomatous loss of the laminar functions in the human lateral geniculate nucleus (LGN) and superior colliculus (SC) remains difficult to detect and poorly understood. Using functional MRI, we measured neural signals from different layers of the LGN and SC, as well as from the early visual cortices (V1, V2 and MT), in patients with early-stage glaucoma and normal controls. Compared to normal controls, early glaucoma patients showed more reduction of response to transient achromatic stimuli than to sustained chromatic stimuli in the magnocellular layers of the LGN, as well as in the superficial layer of the SC. Magnocellular responses in the LGN were also significantly correlated with the degree of behavioral deficits to the glaucomatous eye. Finally, early glaucoma patients showed no reduction of fMRI response in the early visual cortex. These findings demonstrate that 'large cells' in the human LGN and SC suffer selective loss of response to transient achromatic stimuli at the early stage of glaucoma. *Hum Brain Mapp 37:558–569, 2016.*   © 2015 Wiley Periodicals, Inc.

Key words: fMRI; LGN; SC; glaucoma

◆━━━━━━━━━━━━━━━━━━━━━━━━━━━━━━◆

*Correspondence to: Peng Zhang, State Key Laboratory of Brain and Cognitive Science, Institute of Biophysics, Chinese Academy of Sciences, Beijing 100101, China. E-mail: zhangpeng@ibp.ac.cn and Xinghuai Sun, Department of Ophthalmology, Eye and ENT Hospital, Fudan University, Shanghai 200031, China. E-mail: xhsun@shmu.edu.cn

INTRODUCTION

Glaucoma is a neurodegenerative eye disease that affects more than 70 million people worldwide [Quigley and Broman, 2006]. Characterized by gradual loss of retinal ganglion cells and progressive degeneration of the optic nerve, if left untreated, glaucoma results in irreversible vision loss or blindness. Due to transsynaptic degenerations, glaucoma also damages the post-retinal visual system in the human brain, such as the lateral geniculate nucleus (LGN) and V1 [Gupta et al., 2006]. Although the pathology of glaucoma has been extensively studied at the level of retina and optic nerve head ;Crish et al., 2010; El-Danaf and Huberman, 2015; Morgan, 2002; Quigley et al., 1988; Quigley et al., 1987; Weber et al., 1998], the mechanisms of post-retinal neuronal degenerations in the human visual system are not clear, especially at an early stage of the disease. Exploring the early post-retinal mechanisms of glaucoma might be helpful to develop new tools for the diagnosis and treatment of the disease.

The human LGN and superior colliculus (SC) receive direct input from the retina and are the earliest stages in the hierarchy of human visual system. Therefore they are the ideal sites for studying the post-retinal mechanism of neurodegeneration at the early-stage of glaucoma in humans. Previous glaucoma studies on the LGN are mostly based on artificially induced glaucoma in animal models, which may reflect different pathologies from that in humans. In the very few studies on the LGN in human glaucoma patients [Chaturvedi et al., 1993; Gupta et al., 2006, 2009], patients were at an advanced stage of the disease and already suffered severe visual loss, thus what happens to the human LGN at an early stage of the disease is still unknown. To the best of our knowledge, the glaucomatous damage to the primate SC has never been studied before.

Human LGNs and SCs consist of multiple functional layers with different types of neurons. The LGN has six main layers. The inner two layers consist of larger cells and are called the magnocellular (M) layers, which are sensitive to transient achromatic visual information. The outer four layers with smaller cells are called the parvocellular (P) layers, which mainly process sustained chromatic visual information. The human SCs are segregated into superficial, intermediate, and deep layers. The superficial layer receives direct input from the retina ;Leventhal et al., 1981; Perry and Cowey, 1984] and mainly responds to visual stimuli. The intermediate and deep layers are more

Abbreviations

GLM	General linear models
GON	Glaucomatous optic neuropathy
LGN	Lateral geniculate nucleus
MD	Mean defect
POAG	Primary open-angle glaucoma
SAP	Standard automated perimetry
SC	Superior colliculus

related to eye and head movement [Wurtz and Goldberg, 1971], as well as attention shift [Ignashchenkova et al., 2004], receiving cortical inputs from a number of frontal and parietal cortical areas [Fries, 1984].

Different neurons in the functional layers of the LGN and SC might be differentially affected during the progression of glaucoma. Primate glaucoma models and human autopsy studies indicated that the M layers of the LGN were more vulnerable to glaucomatous damage in comparaison to the P layers [Chaturvedi et al., 1993; Gupta et al., 2007; Weber et al., 2000]. Previous studies mainly focused on morphological changes of the LGN, such as cell size, number, density, and layer volume, etc. Functional consequence of glaucoma to different types of neurons in the LGN and SC, especially at an early stage of the disease, remains unknown.

In the present study, we measured fMRI (functional magnetic resonance imaging) signals from the M (inferior) and P (superficial) layers of the LGN, as well as from different depth in the SC of normal controls and early glaucoma patients. Two stimuli (the M and P stimuli) were designed to preferentially active magnocellular neurons in the LGN M layers or parvocellular neurons in the P layers, respectively. Compared to normal controls, early glaucoma patients showed selective signal loss to the M stimulus in the M layers of the LGN as well as in the superficial layer of the SC, but not in the LGN P layers or cortical visual areas.

METHODS

Subjects

Eighteen patients diagnosed with early-stage open-angle glaucoma (age: 33.0 ± 5.6 years, 14 males and four females) and eighteen normal controls (with age and gender exactly matched with the patient group) participated in this study. The patient group included ten primary open-angle glaucoma (POAG) patients and eight normal-tension glaucoma patients, with at least one eye at an early stage of the disease. Visual acuity (20/25 or better) and refractive errors (less than ± 5.00 D sphere and ± 2.00 D cylinder) were approximately matched (less than ± 0.50D sphere differences and/or less than ± 0.25D cylinder differences) between the patient and control groups. None of the patients showed any visual dysfunctions other than glaucoma. All subjects gave written informed consent before the experiments. The ethics committee of Eye & ENT hospital approved the experimental protocol. More detailed subject information was shown in Table I.

Diagnostic criterion was based on glaucomatous optic neuropathy (GON) judged by two glaucoma specialists independently. Inconsistencies between the two specialists were resolved by adjudication from a third glaucoma specialist. Most patients had consistent judges by two glaucoma specialists and only one normal-tension glaucoma patient need to receive a definitive diagnosis by the third

TABLE I. Participants information

	Patient			Normal
	POAG	NTG	Total	
Numbers of participants	10	8	18	18
Numbers of male participants	8	6	14	14
Age (year)	34.2 ± 6.1	31.5 ± 5.0	33.0 ± 5.6	33.0 ± 5.6
Test eye (numbers of OD)	5	5	10	10
Highest IOP of test eye without treatment (mmHg)	27.5 ± 3.4	18.9 ± 1.5	23.7 ± 5.2	–
Highest IOP of test eye during data-collection period (mmHg)	16.2 ± 1.0	11.5 ± 0.5	14.1 ± 2.5	–
MD scores of test eye	1.9 ± 1.2	2.5 ± 1.7	2.2 ± 1.5	–

OD: right eye, MD: mean defect; IOP: intraocular pressure.

specialist. Moreover, during the follow-up period after data-collection phase, the glaucomatous damage progress of the patient confirmed the diagnosis. GON was identified by evidence of any of the following signs: excavation, neuroretinal rim thinning or notching, nerve layer defects, or asymmetry or the vertical cup-to-disc ratio greater than 0.2 between the two eyes. Patients performed Standard Automated Perimetry (SAP) test before the experiment (Octopus 900 perimeter, Haag-Streit USA), G standard white/white TOP program. Reliable visual field results was defined as <= 33% false positives and false negatives, reliable factor >=15% and pupil diameter >=3 mm. Final results determined by repeatable visual field tests of at least two consecutive visits. All patients were free from a history of intraocular surgery, cataract, secondary causes of elevated intraocular pressure (e.g., corticosteroid-induced, trauma, iridocyclitis), other diseases impairing visual field (e.g., pituitary neoplasms, diabetic retinopathy), and any systemic diseases known to affect visual function or M/P pathway function (e.g. migraine). Early-stage of glaucoma was defined according to the Modified Glaucoma Staging System [Mills et al., 2006].

Stimuli and Procedures

Visual stimuli were generated in MATLAB (Mathworks Inc.) with psychophysics toolbox extension [Brainard, 1997; Pelli, 1997], running on a MacBook pro computer, presented by MRI safe projectors at the screen resolution of 1024x768@60Hz.

Figure 1A shows the M and P stimuli that were used to identify the M and P layers of the LGN. The M stimulus was a low spatial frequency sine wave pattern at 30% luminance contrast, and counter phase flickered at 10 Hz. The P stimulus was a high spatial frequency, isoluminant red/green square wave pattern, reversing contrast at 0.5 Hz. The luminance of the red and green color in the P stimulus was matched for each individual with a minimal flicker procedure. Red (RGB values: [128+R 128-G 0]) and green (RGB values: [128-R 128+G 0]) square patches flickered at 30Hz. The amplitude of the red gun (value R) was fixed and subjects adjust the amplitude of the green gun (value G) until the flickering percept reached minimal. The isoluminant adjustment was repeated four times to obtain an average. The M and P stimuli rotated clockwise or counterclockwise (24 degrees/second for the M stimulus and 2.4 degrees/second for the P stimulus) to prevent a signal drop from adaptation. Moving vs. static concentric ring stimuli were used to identify the human homologue of primate MT/V5 (Fig. 1B). The moving ring was presented at 10% contrasts, expanding or contracting at 2.4 degs/second; the static ring was presented at full contrast. The full field M/P stimuli and the ring stimuli subtended 24 degrees of visual angle in diameter. Figure 1C shows the hemifield localizer for the whole LGN. Full contrast hemifield checkerboard stimuli flickered at 7.5 Hz, and presented alternatively to the left or right visual field every 16s. Counter phase flickering wedges were presented sequentially at the vertical (upper/lower) and horizontal (left/right) meridians to identify the boundaries of visual area V1 and V2 on the cortical surface. The ROIs of V1 and V2 were determined as voxels significantly activated by the hemifield localizers within the corresponding V1 and V2 boundaries.

Seven runs were scanned for each subject, consisting of two runs for the LGN hemifield localizer, one run for the MT localizer and four runs for the M/P localizer. Each run collected 162 volumes of images. During the experiments, subjects were instructed to keep central fixation. Subjects viewed the stimuli monocularly with the other eye patched throughout the scanning session. Tested eyes were matched between patients and controls.

MRI Protocol

MRI data were collected with 3T scanner (Siemens Verio) at the Eye and ENT Hospital of Fudan University, using a 12-channel Head Matrix coil. A gradient echo planar imaging sequence was used to acquire functional images (voxel dimension is 2 mm isotropic, 26 axial slices of 2 mm thickness, 64×64 matrix with 2 mm in-plane resolution, TR/TE = 2,000/28 ms, flip angle = 90°). High-
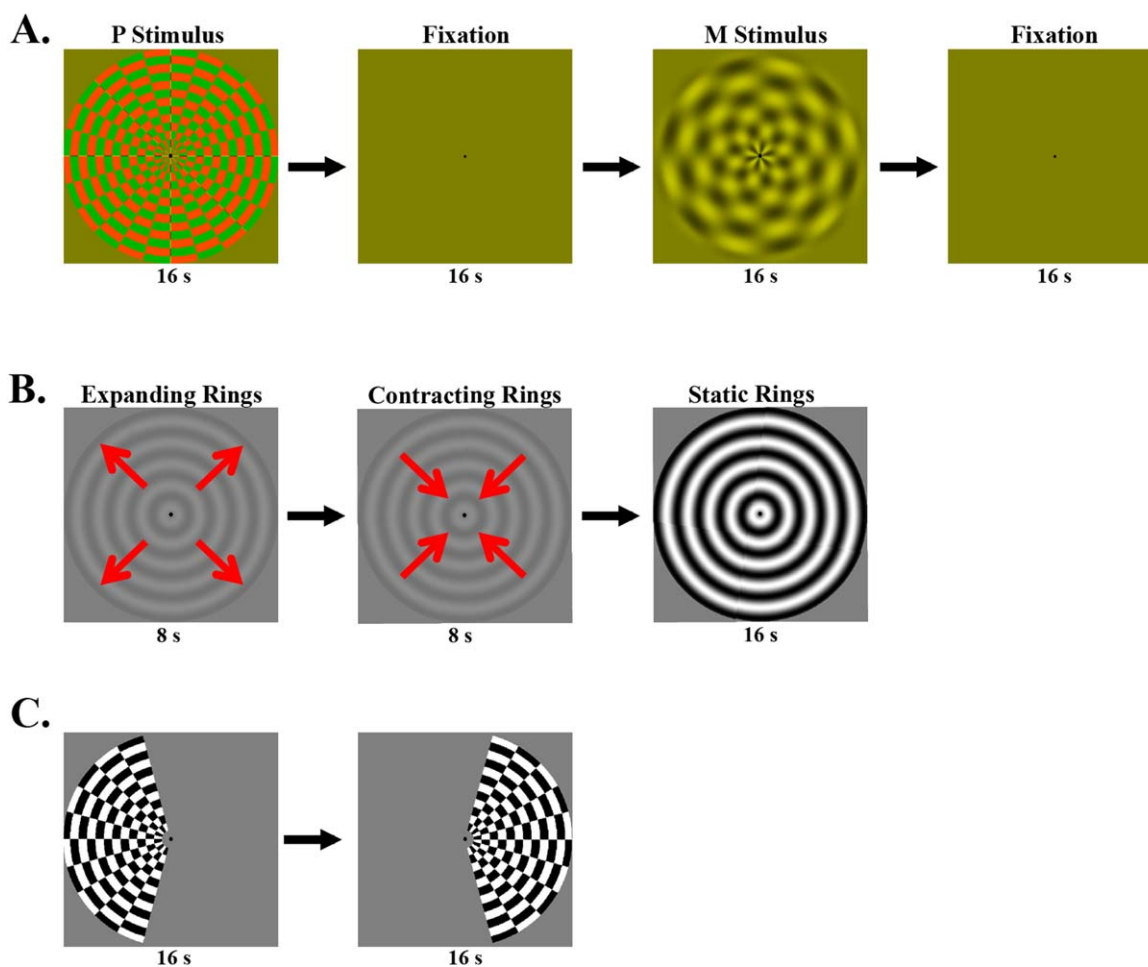
Figure 1.

(**A**) Stimuli for the M and P localizer. The M and P stimuli were presented in blocks of 16 s duration, alternating with 16 s fixation. (**B**) Stimuli for the MT localizer. Each stimulation cycle started with a low contrast ring expanding for 8 s, and then contracting for 8 s, followed by a static ring of high contrast presented for 16 s duration. C. Stimuli for the LGN localizer. The hemifield checkerboards alternatively presented every 16 s between the left and right visual field. [Color figure can be viewed in the online issue, which is available at wileyonlinelibrary.com.]

resolution anatomic volume was obtained with a T1 MPRAGE sequence (1 mm isotropic voxels, 192 sagittal 1 mm thick slices, 256 × 256 matrix with 1 mm in-plane resolution, TR/TE/TI = 2,600/3.02/900 ms, flip angle = 8°). Another high-resolution T2 anatomical scan co-aligned with the functional images was acquired to assist the registration from the T1 anatomical to EPI functional images (TSE T2w sequence, TR/TE = 3,400/89 ms, 26 axial slices with 2 mm thickness, 256 × 256 matrix with 1 mm in-plane resolution, flip angle = 60°).

MRI Data Analysis

MRI data were analyzed using AFNI [Cox, 1996], SPM [Friston, 1996] and custom Matlab code. The first two volumes of each run were discarded to avoid magnetic satu-ration effects. The functional images from each run were first resampled to 1 mm isotropic, realigned to the first image of the first run in this session. There is no signifi-cant difference in head motion between normal controls and glaucoma patients. The high-resolution T1 volume was registered to the T2 anatomical volume, and then normalized to the MNI space. Functional images were nor-malized to the MNI space based on the warping parame-ters estimated from the T1 volume. Linear trend in the fMRI time series were removed, and the unit of the time series was converted to percent signal change.

The beta values of different stimulus conditions were fit-ted and extracted with general linear models (GLM), the six parameters from motion registration were included in the GLM as noise regressors. The ROIs of the LGN were defined from the activation map of the hemifield localizer
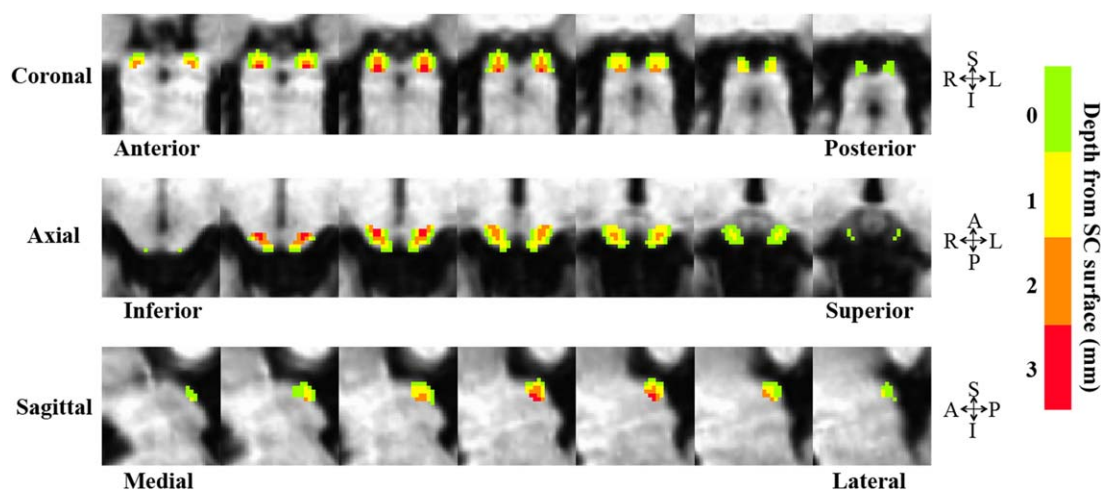
Figure 2.
ROIs of different depth from the surface of the SC. [Color figure can be viewed in the online issue, which is available at wileyonlinelibrary.com.]

and T1 anatomical images. Care was taken not to include activations from the pulvinar nuclei, which located more posterior and medial than that of the LGN. Our recent paper shows more details about the ROI definition of the LGN [Zhang et al., 2015]. Beta values in the LGNs were extracted and analyzed in Matlab. The coordinates of the right LGNs were mirror flipped to the left, and then the coordinates for all LGNs were aligned to their mass center (by subtracting the coordinate of the LGN center). Group average of the beta values and T statistics were generated from the registered LGNs. Similar approaches were used to analyze the data from the SC, except that the ROIs of the SC were defined from T1 anatomical images. The upsampling procedure provided a better estimation of the center of the LGN and improved the averaged results, which helped to resolve the magnocellular and parvocellular layers of the LGN. Since the sampling window (about $8 \times 6 \times 6$ mm FOV in 2 mm isotropic resolution) for each LGN is slightly different in position, the upsampling (to 1 mm isotropic voxels) and averaging approach is equivalent (when the number of averages is large enough) to convolving the high-resolution LGN image (1 mm resolution) with a 2 mm cubic filter. This 2 mm low pass filter cannot resolve individual layers of the LGN, but is small enough to differentiate the M and P sections (both are larger than 2 mm in each dimension) and also improves SNR.

ROIs of Different Depth in the SC

Figure 2 shows the ROIs of different depths from the surface of the SC. With the drawing tools in AFNI, we first defined the surface voxels, whose depth was 0 mm. Then the depth for each voxel in the SC was calculated as the shortest distance from the voxel to all surface voxels.

RESULTS

Selective Reduction of fMRI Response to the M Stimulus in the M Layers of the Patient LGN

Figure 1A shows the M and P stimulus designed to preferentially activate the neuronal responses in the magnocellular and parvocellular layers of the LGN. The P stimulus was a high spatial frequency and high chromatic contrast checkerboard, which counterphase flickered at a low temporal frequency. While the M stimulus was a low spatial frequency and low luminance contrast checkerboard, flickered at a high temporal frequency.

Figure 3A shows the LGN voxels that were preferentially activated by the M or P stimulus. In the LGNs of healthy controls, two clusters of voxels can be clearly identified. One of the clusters was located more inferior and anterior, and showed stronger response to the M stimulus than to the P stimulus. In the present study, we labeled this functional subdivision with response bias to the M stimulus as the M layers of the LGN. The other cluster with stronger response to the P stimulus was located more superior and posterior, and was defined as the P layers of the LGN. The topography of the M and P layers is highly consistent with another study from our group, which used the same stimuli but a different group of subjects and a different MRI scanner [Zhang et al., 2015]. The spatial relationship between the M and P layers is consistent with the anatomy of the human LGN (please refer to Figure 3 of the previous paper [Zhang et al., 2015] for comparison with the LGN anatomy from autopsy brain slices). This study also found distinct response properties of the M and P layers with stimuli varying in spatio-temporal frequency, contrast and chromaticity, which is consistent with the non-human primate physiological evidence. Another
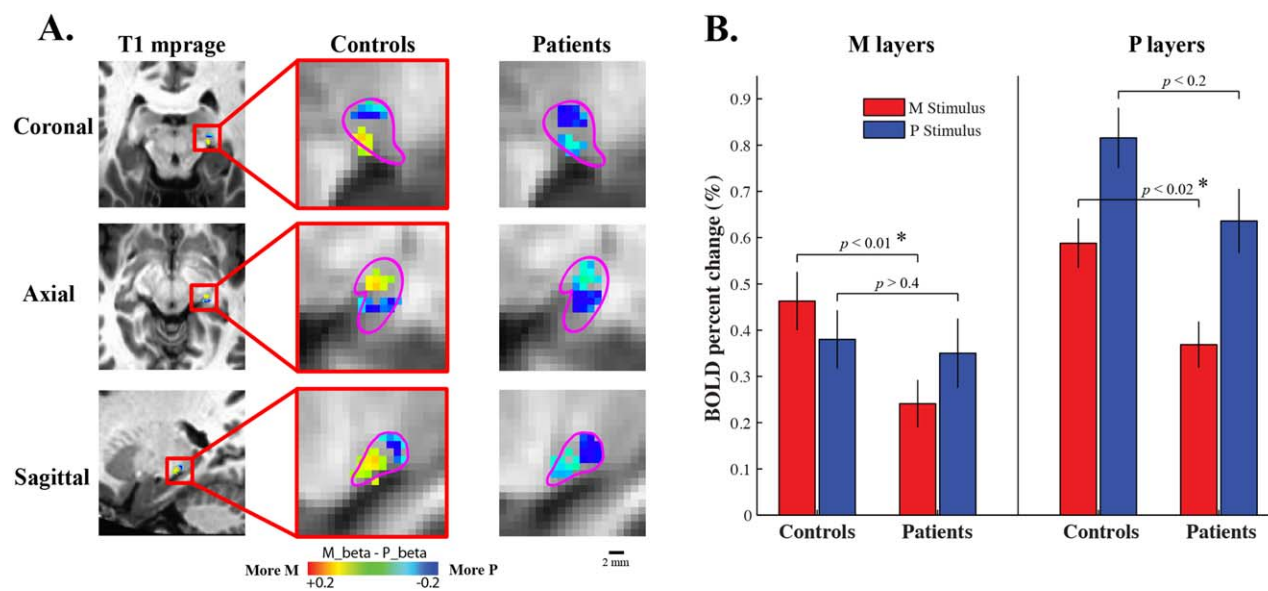
Figure 3.

(**A**) The M and P layers of the LGNs of normal controls and glaucoma patients. The M layers were identified as 30 voxels with strongest bias to the M stimulus, while the P layers were defined as 30 voxels with strongest bias to the P stimulus. Purple lines illustrate the boundary of the LGN from anatomical images. Red/yellow indicates voxels with greater responses to the M stimulus than to the P stimulus, and voxels having greater responses to the P stimulus were shown by blue/cyan. The topography of the M and P layers was consistent with the LGN anatomy from autopsy brain slices, which were shown in our recent paper [Zhang et al., 2015]. (**B**) FMRI responses to the M and P stimuli in the M and P layers of the LGNs of normal controls and glaucoma patients. Error bars indicate standard error of the mean across ROIs. [Color figure can be viewed in the online issue, which is available at wileyonlinelibrary.com.]

research group used different M/P stimuli as well as different scanning procedures to identify the M and P layers of the LGN [Denison et al., 2014], and found very similar spatial patterns as in our studies. In the present study, the M and P layers of the LGN are identified as voxels showing response bias, rather than exclusive responses, to the M or to the P stimulus. In other words, the M (P) voxels also responded to the P (M) stimulus, but more weakly than to the M (P) stimulus. This is not surprising for two reasons: first, the neuronal responses in the M and P layers are preferentially rather than exclusively tuned to the M and P stimuli; and second, the spatial specificity of fMRI signal is relatively low, so the response of M voxels very likely included contributions from both M and P cells, though more from the M cells than P cells.

In the LGNs of glaucoma patients (shown by the third column in Fig. 3A), nearly all the voxels responded stronger to the P stimulus, and no cluster of voxels showing stronger response to the M stimulus can be found. Figure 6 shows the averaged fMRI response of all LGN voxels. Compared to normal controls, the LGNs of glaucoma patients produced significantly reduced response to the M stimulus, but not to the P stimulus. These findings indicate that there is a selective reduction of response to transient achromatic stimulus (or the M stimulus) in the LGNs of early glaucoma patients. In order to investigate M/P layer-specific response of the patient LGNs, the P layers were defined as voxels with most negative M-P beta values, which is the same approach as used to identify the P layers of normal controls. While the M layers were defined as voxels with least negative M-P beta values, mathematically, this M voxels selection criterion is equivalent to the M voxels selection criterion used for normal controls (selecting the most positive M-P beta values). The same approach has been used in Denison et al.'s study [Denison et al., 2014], which showed reliable segmentations of the M and P layers of the LGN. In the current study, the M voxels of the patient LGNs (with least negative M-P beta values) formed a continuous cluster, which is located more anterior and posterior relative to the P cluster (with most negative M-P beta values). The M/P layer topography of the patient LGNs is highly consistent with that found for normal controls (Fig. 3A), and also consistent with the segmentation results from previous studies [Denison et al., 2014; Zhang et al., 2015]. The mass centers of the M and P layers and spatial gradient of the M/P beta maps are highly consistent in the LGNs of controls and patients (supplemental Figure S2, individual M-P beta maps were shown by Figure S3). Therefore, these data shows that the M and P layers of the LGN can be

successfully identified in both normal controls and glaucoma patients, which provide an opportunity to further investigate early glaucomatous change in different functional layers of the LGN.

Figure 3B shows the M/P layer-specific fMRI response to the M and P stimulus in the LGNs of controls and patients. In the LGN M layers, a significant two-way interaction can be found between stimuli (M/P stimuli) and groups (controls/patients), $F(1,70) = 5.3$, $p < 0.03$. Specifically, the fMRI response to the M stimulus was significantly reduced in glaucoma patients compared to normal controls [$t(70) = -2.69$, $p < 0.01$], while the fMRI response to the P stimulus showed no significant difference between the two groups [$t(70) = -0.24$, $p > 0.4$]. These results indicate that in the M layers of the LGN, there is a selective response loss to the M stimulus but not to the P stimulus. In the LGN P layers, there was no significant interaction between stimuli and groups [$F(1,70) = 0.29$, $p > 0.5$], suggesting that in the P layers of the patient LGNs, there is no selective loss of response to the M or to the P stimulus. Specifically, compared to normal controls, the P layers' response to the M stimuli was significantly reduced in the patient group [$t(70) = -2.51$, $P < 0.02$], and the P layers' response to the P stimulus showed a non-significant trend of reduction [$t(70) = -1.53$, $P < 0.2$]. Our data showed stronger fMRI response in the P layers than in the M layers ($F(1,70) = 67.9$, $P < 0.001$), which might be due to greater partial volume effect to the M layers' response (smaller volume than the P layers). These responsive P voxels might be generally more sensitive to visual stimulation, which could explain their general loss of signals to both the M and P stimulus. To summarize, our data shows that in the LGNs of early glaucoma patients, compared to normal controls, there is a selective response loss to the M stimulus in the M layers, while the P layers show a general loss of response to both M and P stimulus. This finding is further supported by a significant three-way interaction between stimuli, layers (M/P layers) and groups [$F(1,70) = 6.04$, $P < 0.02$].

It may appear that the layer-specific response profiles are predetermined by the voxel selection criterion [Kriegeskorte et al., 2009]: selecting the layer voxels via response bias to the M/P stimulus and then analyzing the responses to the M/P stimulus in these voxels. Indeed, the primary emphasis here is not that M/P voxels responded more strongly to M/P-biased stimulus, rather the key finding is that using the same voxel selection criterion in controls and patients, and with the resulting layer segmentation highly consistent between these two groups of subjects, our results show a significant and selective response deficit to the M stimulus from the M layers in the patient group. In addition, the M and P layers identified in this study are highly consistent with the results from other studies using independent datasets [Denison et al., 2014; Zhang et al., 2015]. Importantly, the key aspect of the results, that there is a deficiency in responding to the M stimulus in the patients' LGNs, is not a product of LGN voxel classification, as the deficient response to M stimulus could already be seen in the average response of the entire LGN. In a further analysis, the fMRI data was randomly split in half, one half was used to identify the M and P layers and the other half was used for ROI-based analysis, and we found similar results as in Figure 3.

Recent MRI studies found shrinkage of LGNs for advanced glaucoma patients [Gupta et al., 2009], and the LGN volume was well correlated with the thickness of retinal nerve fiber layer and perimetric loss [Chen et al., 2013; Dai et al., 2011; Gupta et al., 2009; Zhang et al., 2012]. To investigate whether significant LGN atrophy could occur even at the early stage of glaucoma, we compared the LGN volume of normal controls and early glaucoma patients. The volume of the LGNs was measured as significant activations by the hemifield localizer from the anatomical location of the LGN (based on T1 images). We were very careful not to include activations from the pulvinar nuclei, which located more posterior and medial than that of the LGN. The LGN volume for the glaucoma patients was 158 ± 26 mm^3 (mean ± SD), which was significantly smaller compared to the LGNs of normal controls (177 ± 22 mm^3, $t(70) = -3.4$, $P < 0.002$). This finding indicates that even at the early stage of glaucoma, significant LGN atrophy could occur.

Severity of Early Glaucoma Correlates with fMRI Response in the LGN M Layers

All glaucoma patients received standard automatic perimetry (SAP) test. The mean defect (MD), a parameter from the SAP, serves as an index for the severity of glaucoma. In Fig. 4, the normalized M layers response of a single LGN (the fMRI response in the M layers minus that in the P layers) was drawn as a function of behavioral deficit in the corresponding visual field. Figure 4A shows that across different LGNs of glaucoma patients, the relative measure of M layer response to the M stimulus significantly correlated with the severity of glaucoma in the corresponding visual field of the LGNs ($r = -0.46$, $P < 0.01$). In other words, if the hemi visual field contains greater behavioral deficits from glaucoma, the M layers of the contralateral LGN are less responsive to visual stimulation compared to the P layers. Consistent with the negative correlation with the M layers response to the M stimulus, the behavioral deficits of glaucoma to the corresponding hemifield also showed a non-significant trend of negative correlation with the normalized M layers response to the P stimulus (Fig. 4B, $r = -0.19$, $P = 0.28$). These findings indicate that the weaker fMRI response (especially to the M stimulus) in the M layers compared to that in the P layers, the more severe visual deficit from early glaucoma.

Reduced fMRI Response to the M Stimulus in the Superficial Layer of the Patient SC

The superficial layer of SC receives direct input from the retina, in particular of the parasol (magnocellular) ganglion cell type [Crook et al., 2008], and the M but not the
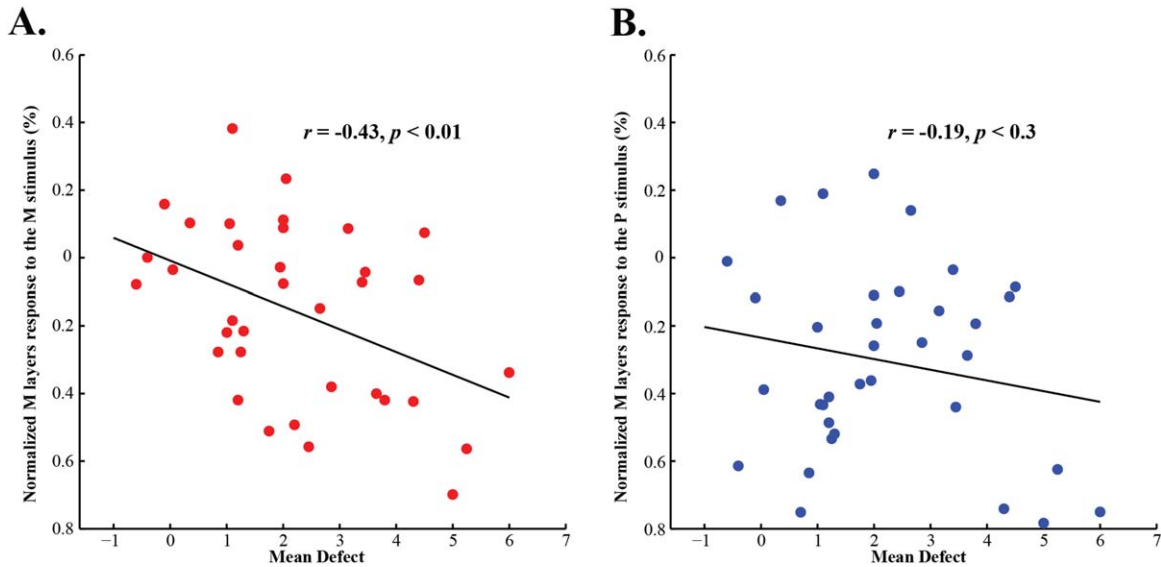
A.

$r = -0.43, p < 0.01$

B.

$r = -0.19, p < 0.3$

Figure 4.

Correlation between the severity of glaucoma and normalized M layers response to the M and P stimuli. X-axis corresponds to the severity of glaucoma, the Mean Defect (MD), a summary perimetric measure. Y-axis indicates the difference between responses in the M layers and P layers of the LGN, a normalized measure of the M layers response to the M and P stimuli. (**A**) There is a significant negative correlation between the severity of glaucoma and the normalized M layers response to the M stimulus ($r = -0.46$, $P < 0.01$). (**B**) There is a non-significant trend of negative correlation between the severity of glaucoma and the normalized M layers response to the P stimulus ($r = -0.19$, $P < 0.3$). [Color figure can be viewed in the online issue, which is available at wileyonlinelibrary.com.]
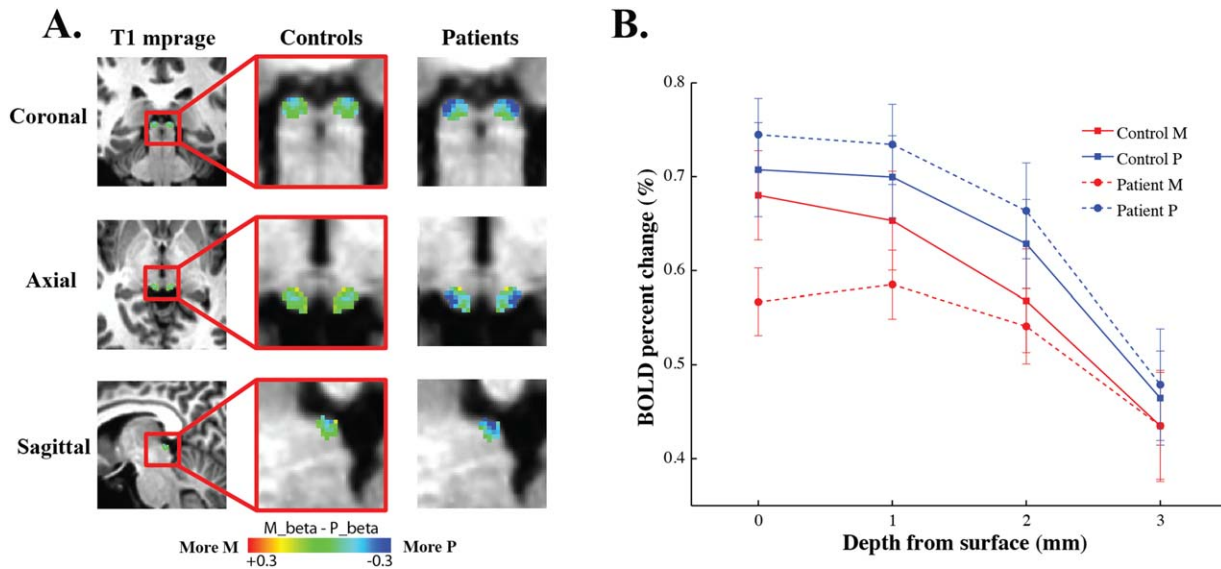

Figure 5.

fMRI responses to the M and P stimuli in the SC of normal controls and glaucoma patients. (**A**) The M-P beta maps in the SC. The left column shows the anatomical location of the SC in coronal, axial and sagittal planes of a middle section of the brain. The middle and right columns show the M-P beta maps in the SC of normal controls and glaucoma patients, respectively. (**B**) SC responses to the M and P stimuli as a function of voxel's depth from the surface of the SC. Red and blue lines indicate response to the M and P stimulus, respectively. Solid and dashed lines represent responses from normal controls, and glaucoma patients respectively. [Color figure can be viewed in the online issue, which is available at wileyonlinelibrary.com.]
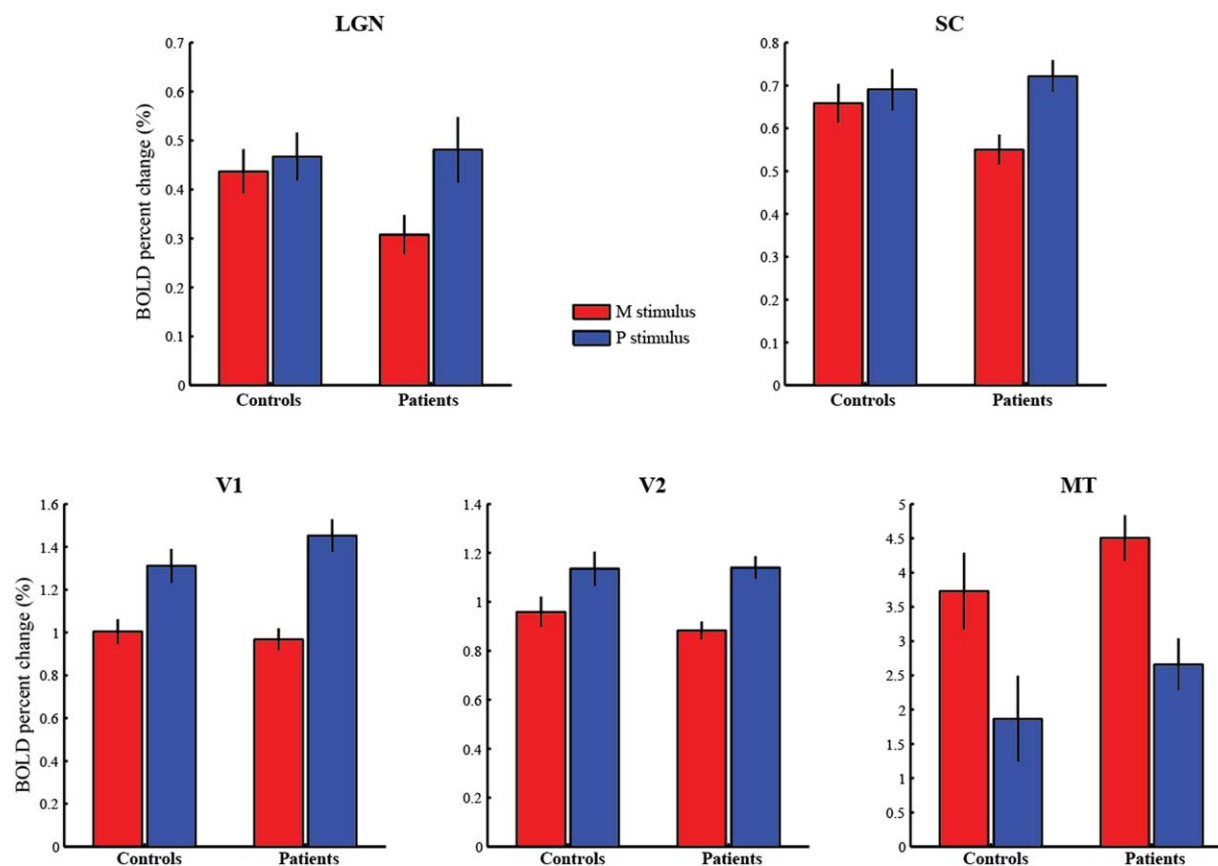
Figure 6.

FMRI responses to the M and P stimuli in the subcortical nuclei (LGN and SC) and cortical visual areas (V1, V2 and MT). Comparing to normal controls, glaucoma patients showed selective loss of fMRI response to the M stimulus in the LGN and SC, but not in V1, V2 or MT. [Color figure can be viewed in the online issue, which is available at wileyonlinelibrary.com.]

P layers of the LGN project to the SC indirectly through a corticotectal pathway [Hoffmann, 1973]. Also, fMRI measured responses in the SC saturate at very low luminance contrast [Schneider and Kastner, 2005], which is very similar to the contrast response property of the magnocellular layers of the LGN. Figure 5 shows that the fMRI response of the SC to the visual stimuli gradually decreases as a function of depth from the surface of the SC (Fig. 2 shows the depth map of the SC), which is consistent with the fact that the superficial layer is mostly composed of visual sensory neurons. This finding is also consistent with recent fMRI studies on the SC showing that high contrast visual stimuli evoked strongest response in the superficial layer of the SC [Katyal and Ress, 2014; Zhang et al., 2015]. FMRI signals measured at the superficial voxels (depth = 0 mm) showed a significant interaction between stimulus conditions (M/P stimuli) and subject groups (controls/patients) [$F_{(1,70)} = 5.94$, $P < 0.02$]. Specifically, the responses to the M stimulus were considerably reduced in glaucoma patients compared to normal controls, but no significant difference was found between patients and controls in

responses to the P stimulus. These results indicate early glaucomatous loss of the magnocellular responses in the superficial layers of the human SC, similar to the results found in the magnocellular layers of the LGN.

No Glaucomatous Loss of fMRI Response in the Visual Cortex

Figure 6 shows the average fMRI response to the M and P stimuli in the subcortical visual nuclei LGN and SC, as well as in the cortical visual areas V1, V2 and MT of normal controls and glaucoma patients. The average response in the LGN showed a significant interaction between stimuli (M/P stimuli) and groups (controls/patients), $F_{(1,70)} = 5.14$, $P < 0.03$. Specifically, the LGN response to the M stimulus was significantly reduced in glaucoma patients compared to normal controls [$t_{(70)} = -2.10$, $P < 0.05$], while no reduction was found to the LGN response to the P stimulus [$t_{(70)} = 0.17$, $P > 0.8$]. The fMRI response in the SC also showed a significant interaction between stimuli and groups: $F_{(1,70)} = 5.38$, $P < 0.03$. The M response

showed a trend of reduction in the patient group [t (70) = −1.89, $P < 0.07$], and the P response showed no significant difference between the two groups [t (70) = 0.5, $P > 0.6$]. These findings indicate selective reduction of fMRI response to transient achromatic stimulus (M stimulus) in the LGN and SC of early glaucoma patients.

The fMRI response in V1 was stronger to the P stimulus than to the M stimulus (main effect of stimuli: F (1,30) = 83.12, $P < 0.001$; main effect of groups: F (1,30) = 0.37, $P > 0.5$). A significant interaction can be found between stimuli and groups [F (1,30) = 4.21, $P < 0.05$]. The P response showed a trend of increment in the patient group [t (70) = 1.29, $P < 0.21$], the M response showed no significant difference between the two groups [t (70) = −0.47, $P > 0.6$]. The fMRI response in V2 also showed stronger response to the P stimulus than to the M stimulus (main effect of stimuli: F (1,30) = 42.12, $P < 0.001$; main effect of groups: F (1,30) = 0.25, $P > 0.6$], but no significant interaction was found between stimuli and groups [F (1,30) = 1.45, $P > 0.2$]. In MT, the fMRI response was significantly stronger to the M stimulus than to the P stimulus [main effect of stimuli: F (1,30) = 92.8, $P < 0.001$], and showed a trend of increment in the patient group [main effect of groups: F (1,30) = 1.38, $P < 0.3$]. However, unlike the M layers of the LGN and the superficial layer of the SC, there is no significant interaction between stimuli and groups (F (1,34) = 0.002, $P > 0.9$). In summary, compared to normal controls, early glaucoma patients showed selective reduction of fMRI response to the M stimulus in the LGN and SC, but not in the cortical visual areas V1, V2 and MT. The fMRI response in V1 and MT showed a small trend of increment in the patient groups, which is likely to be a result of neural compensation at the cortical level.

DISCUSSION

Transsynapic degeneration is a common phenomenon in the human early visual system when the visual input was deprived at the level of retina or optic nerves [Barcella et al., 2010; Beatty et al., 1982; Boucard et al., 2009; Ciccarelli et al., 2005; Ogawa et al., 2014]. Early glaucomatous neurodegeneration in the subcortical visual nuclei remains poorly understood. In the present study, we measured fMRI signals from the magnocellular and parvocellular layers of the LGN, as well as from different depths in the SCs of early glaucoma patients and normal controls. Compared to normal controls, early glaucoma patients showed reduced fMRI response in the LGN with functional and anatomical specificity: there was greater loss of response to the M stimulus than that to the P stimulus, which was found only in the magnocellular layers but not in the parvocellular layers of the LGN. Also, the visual deficits from glaucoma showed a significant negative correlation with the fMRI responses to the M stimulus in the M layers of the LGN. Similar to the LGN M layers, the superficial

layer of the SC of early glaucoma patients also showed significantly reduced fMRI response to the M stimulus but not to the P stimulus. Furthermore, there is no glaucomatous loss of fMRI response in the early visual areas V1, V2 and MT. We found no significant difference between the POAG patients and normal-tension glaucoma patients (Supplemental Figure S1).

Reduced fMRI Response to the M Stimulus in the M Layers of the LGN

Primate glaucoma models suggest that larger cells in the early visual system are more susceptible to glaucomatous damage than smaller cells. On the retina, parasol cells showed more atrophy and losses than midget cells [Morgan, 2002; Weber et al., 1998]. Large optic nerve fibers also underwent faster atrophy and greater losses than smaller fibers [Yucel et al., 2001, 2003]. But in the LGN, existing pathological evidence is not consistent. Primate glaucoma models found more cell losses and dentritic damage in the magnocellular layers than those in the parvocellular layers of the LGN [Gupta et al., 2007; Weber et al., 2000], which is consistent with the pathological findings on the retina. However, neurons in the P layers also showed greater atrophy than those in the M layers [Yucel et al., 2001], and increased cell densities [Weber et al., 2000]. Besides, the functional changes to neurons in the M and P layers of the LGN are not clear. One study showed that the neural metabolism in the LGNs of experimental primate glaucoma was reduced to the same degree in the M and P layers [Crawford et al., 2000]. Since animal models of glaucoma induced with elevated IOP (intraocular pressure) may produce different pathologies to human glaucoma, human studies are necessary to correctly understand the etiology in humans.

Human glaucoma studies on the LGN are very few and focused on morphological changes. The only human autopsy study showed reduced cell density in the M layers but not in the P layers of the LGN for patients with advanced glaucoma [Chaturvedi et al., 1993]. A structural MRI study showed atrophy of the whole volume of the patient LGN [Gupta et al., 2009], without further segmentation of the M and P layers. Therefore, before the current study, functional changes to the M and P layers of the human LGN during early glaucoma are not clear.

Our data clearly showed that early glaucoma in humans caused selective loss of magnocellular response in the LGN. There was greater loss of neural activities to the M stimulus than to the P stimulus, which was found only in the M layers but not in the P layers of the patient LGNs. Also, compared to the response in the P layers, weaker fMRI response in the LGN M layers was associated with greater behavioral deficits in the contralateral visual field. These functional data provide strong evidence that early glaucoma causes selective loss of magnocellular functions in the human LGN. The response loss in the LGN M

layers could be due to reduced input signals from the parasol ganglion cells on the retina. However, since we also found significant volume shrinkage of the patient LGNs (to a smaller degree compared to previous studies), the signal loss could also be caused by neuronal degeneration or loss of neuronal responsiveness in the LGN M layers.

Reduced fMRI Response to the M Stimulus in the Superficial Layer of the SC

Although there have been many glaucoma-related studies on the primate LGN, glaucomatous neurodegeneration to the human SC remains unknown. In the present study, we measured neural signals from different depth in the human SC. Voxels in the superficial layer of the SC showed the strongest response to visual stimuli, which is consistent with primate physiology and recent fMRI studies [Katyal and Ress, 2014; Katyal et al., 2010]. In glaucoma patients, the superficial voxels showed significant reduction of fMRI response to the M stimulus but not to the P stimulus (Fig. 4), which is consistent with the pattern of response from the M layers of the LGN. Thus for the first time, we show that at early stage of glaucoma, visual sensory neurons in the superficial layer of the human SC suffered loss of response to transient achromatic stimulus.

No Reduction of fMRI Response in the Early Visual Cortex

Although we found glaucomatous loss of responses to the M stimulus in the LGN and SC, the data showed no response loss either to the M stimulus or to the P stimulus in the cortical visual areas V1, V2 and MT (Fig. 4). These findings suggest that during the early progression of glaucoma, neuronal degenerations might occur in the subcortical visual nuclei before reaching the early visual cortex. The neural responses in V1 and MT slightly increased in the patient group, which might be a result of neural compensation at the cortical level, such as increased contrast gain or response gain to neural signals from the glaucomatous eye.

CONCLUSIONS

The ability to measure layer-specific neural signals noninvasively in the human LGN and SC provides an opportunity to investigate the functional properties of these subcortical nuclei during early-stage glaucoma. Patients showed greater response loss to the M stimulus than to the P stimulus, which was restricted to the magnocellular layer of the LGN, as well as in the superficial layer of the SC. No glaucomatous loss of response was found in the early visual areas. To conclude, early-stage glaucoma causes selective functional loss to 'large cells' in the human LGN and SC, specifically to luminance stimulus modulated at high temporal frequencies.

REFERENCES

Barcella V, Rocca MA, Bianchi-Marzoli S, Milesi J, Melzi L, Falini A, Filippi M (2010): Evidence for retrochiasmatic tissue loss in Leber's hereditary optic neuropathy. Hum Brain Mapp 31: 1900–1906.

Beatty RM, Sadun AA, Smith L, Vonsattel JP, Richardson EP Jr. (1982): Direct demonstration of transsynaptic degeneration in the human visual system: A comparison of retrograde and anterograde changes. J Neurol Neurosurg Psychiatry 45:143–146.

Boucard CC, Hernowo AT, Maguire RP, Jansonius NM, Roerdink JB, Hooymans JM, Cornelissen FW (2009): Changes in cortical grey matter density associated with long-standing retinal visual field defects. Brain 132:1898–1906.

Brainard DH (1997): The psychophysics toolbox. Spat Vis 10:433–436.

Chaturvedi N, Hedley-Whyte ET, Dreyer EB (1993): Lateral geniculate nucleus in glaucoma. Am J Ophthalmol 116:182–188.

Chen WW, Wang N, Cai S, Fang Z, Yu M, Wu Q, Gong Q (2013): Structural brain abnormalities in patients with primary open-angle glaucoma: A study with 3T MR imaging. Invest Ophthalmol Vis Sci 54:545–554.

Ciccarelli O, Toosy AT, Hickman SJ, Parker GJ, Wheeler-Kingshott CA, Miller DH, Thompson AJ (2005): Optic radiation changes after optic neuritis detected by tractography-based group mapping. Hum Brain Mapp 25:308–316.

Cox RW (1996): AFNI: Software for analysis and visualization of functional magnetic resonance neuroimages. Comput Biomed Res 29:162–173.

Crawford ML, Harwerth RS, Smith EL III, Shen F, Carter-Dawson L (2000): Glaucoma in primates: Cytochrome oxidase reactivity in parvo- and magnocellular pathways. Invest Ophthalmol Vis Sci 41:1791–1802.

Crish SD, Sappington RM, Inman DM, Horner PJ, Calkins DJ (2010): Distal axonopathy with structural persistence in glaucomatous neurodegeneration. Proc Natl Acad Sci USA 107:5196–5201.

Crook JD, Peterson BB, Packer OS, Robinson FR, Gamlin PD, Troy JB, Dacey DM (2008): The smooth monostratified ganglion cell: Evidence for spatial diversity in the Y-cell pathway to the lateral geniculate nucleus and superior colliculus in the macaque monkey. J Neurosci 28:12654–12671.

Dai H, Mu KT, Qi JP, Wang CY, Zhu WZ, Xia LM, Morelli JN (2011): Assessment of lateral geniculate nucleus atrophy with 3T MR imaging and correlation with clinical stage of glaucoma. AJNR Am J Neuroradiol 32:1347–1353.

Denison RN, Vu AT, Yacoub E, Feinberg DA, Silver MA (2014): Functional mapping of the magnocellular and parvocellular subdivisions of human LGN. Neuroimage 102:358–369.

El-Danaf RN, Huberman AD (2015): Characteristic patterns of dendritic remodeling in early-stage glaucoma: Evidence from genetically identified retinal ganglion cell types. J Neurosci 35: 2329–2343.

Fries W (1984): Cortical projections to the superior colliculus in the macaque monkey: A retrograde study using horseradish peroxidase. J Comp Neurol 230:55–76.

Friston KJ (1996): Statistical Parametric Mapping and Other Analysis of Functional Imaging Data. Brain Mapping: The Methods. Academic Press. pp 363–385.

Gupta N, Ang LC, Noel de Tilly L, Bidaisee L, Yucel YH (2006): Human glaucoma and neural degeneration in intracranial optic nerve, lateral geniculate nucleus, and visual cortex. Br J Ophthalmol 90:674–678.

Gupta N, Ly T, Zhang Q, Kaufman PL, Weinreb RN, Yucel YH (2007): Chronic ocular hypertension induces dendrite pathology in the lateral geniculate nucleus of the brain. Exp Eye Res 84:176–184.

Gupta N, Greenberg G, de Tilly LN, Gray B, Polemidiotis M, Yucel YH (2009): Atrophy of the lateral geniculate nucleus in human glaucoma detected by magnetic resonance imaging. Br J Ophthalmol 93:56–60.

Hoffmann KP (1973): Conduction velocity in pathways from retina to superior colliculus in the cat: A correlation with receptive-field properties. J Neurophysiol 36:409–424.

Ignashchenkova A, Dicke PW, Haarmeier T, Thier P (2004): Neuron-specific contribution of the superior colliculus to overt and covert shifts of attention. Nat Neurosci 7:56–64.

Katyal S, Ress D (2014): Endogenous attention signals evoked by threshold contrast detection in human superior colliculus. J Neurosci 34:892–900.

Katyal S, Zughni S, Greene C, Ress D (2010): Topography of covert visual attention in human superior colliculus. J Neurophysiol 104:3074–3083.

Kriegeskorte N, Simmons WK, Bellgowan PS, Baker CI (2009): Circular analysis in systems neuroscience: The dangers of double dipping. Nat Neurosci 12:535–540.

Leventhal AG, Rodieck RW, Dreher B (1981): Retinal ganglion cell classes in the Old World monkey: Morphology and central projections. Science 213:1139–1142.

Mills RP, Budenz DL, Lee PP, Noecker RJ, Walt JG, Siegartel LR, Doyle JJ (2006): Categorizing the stage of glaucoma from pre-diagnosis to end-stage disease. Am J Ophthalmol 141:24–30.

Morgan JE (2002): Retinal ganglion cell shrinkage in glaucoma. J Glaucoma 11:365–370.

Ogawa S, Takemura H, Horiguchi H, Terao M, Haji T, Pestilli F, Masuda Y (2014): White matter consequences of retinal receptor and ganglion cell damage. Invest Ophthalmol Vis Sci 55:6976–6986.

Pelli DG (1997): The VideoToolbox software for visual psychophysics: Transforming numbers into movies. Spat Vis 10:437–442.

Perry VH, Cowey A (1984): Retinal ganglion cells that project to the superior colliculus and pretectum in the macaque monkey. Neuroscience 12:1125–1137.

Quigley HA, Broman AT (2006): The number of people with glaucoma worldwide in 2010 and 2020. Br J Ophthalmol 90: 262–267.

Quigley HA, Sanchez RM, Dunkelberger GR, L'Hernault NL, Baginski TA (1987): Chronic glaucoma selectively damages large optic nerve fibers. Invest Ophthalmol Vis Sci 28:913–920.

Quigley HA, Dunkelberger GR, Green WR (1988): Chronic human glaucoma causing selectively greater loss of large optic nerve fibers. Ophthalmology 95:357–363.

Schneider KA, Kastner S (2005): Visual responses of the human superior colliculus: A high-resolution functional magnetic resonance imaging study. J Neurophysiol 94:2491–2503.

Weber AJ, Kaufman PL, Hubbard WC (1998): Morphology of single ganglion cells in the glaucomatous primate retina. Invest Ophthalmol Vis Sci 39:2304–2320.

Weber AJ, Chen H, Hubbard WC, Kaufman PL (2000): Experimental glaucoma and cell size, density, and number in the primate lateral geniculate nucleus. Invest Ophthalmol Vis Sci 41:1370–1379.

Wurtz RH, Goldberg ME (1971): Superior colliculus cell responses related to eye movements in awake monkeys. Science 171: 82–84.

Yucel YH, Zhang Q, Weinreb RN, Kaufman PL, Gupta N (2001): Atrophy of relay neurons in magno- and parvocellular layers in the lateral geniculate nucleus in experimental glaucoma. Invest Ophthalmol Vis Sci 42:3216–3222.

Yucel YH, Zhang Q, Weinreb RN, Kaufman PL, Gupta N (2003): Effects of retinal ganglion cell loss on magno-, parvo-, konio-cellular pathways in the lateral geniculate nucleus and visual cortex in glaucoma. Prog Retin Eye Res 22:465–481.

Zhang YQ, Li J, Xu L, Zhang L, Wang ZC, Yang H, Jonas JB (2012): Anterior visual pathway assessment by magnetic resonance imaging in normal-pressure glaucoma. Acta Ophthalmol 90:e295–e302.

Zhang P, Zhou H, Wen W, He S (2015): Layer-specific response properties of the human lateral geniculate nucleus and superior colliculus. Neuroimage 111:159–166.